Lack of VMP1 impairs hepatic lipoprotein secretion and promotes non-alcoholic steatohepatitis

Xiaoxiao Jiang, Sam Fulte, Fengyan Deng, Shiyuan Chen, Yan Xie, Xiaojuan Chao, Xi C He, Yuxia Zhang, Tiangang Li, Feng Li, Colin McCoin, E. Matthew Morris, John Thyfault, Wanqing Liu, Linheng Li, Nicholas O. Davidson, Wen-Xing Ding, Hong-Min Ni

Table of contents

Supplemental materials and methods

Reagents and antibodies

Antibodies and reagents used in this study are listed in CTAT table.

Hepatic triglyceride and cholesterol analysis

Hepatic lipid extraction was performed as described previously[1]. Frozen liver tissues (20-50 mg) were grinded into powder using a mortar and pestle followed by chloroform-methanol extraction. TG and CHL analysis of lipid extracts was performed using GPO-Triglyceride Reagent Set and Cholesterol liquid reagent (#T7532 and #C7510 respectively, Pointe Scientific, Canton, MI) following the manufacturer's instruction.

In vivo VLDL secretion assay

In vivo VLDL secretion assay was performed as previously described[2]. Mice were fasted for 4 hours prior to tyloxapol 500 mg/kg i.v. or Pluronic™ F-127 10mg/kg in 0.9% NaCl i.p. Tyloxapol or Pluronic™ F-127 inhibits both the lipolysis and tissue uptake of lipoproteins in mice. Blood samples were collected pre-injection and hourly up to 4 hours after injection. TG concentration was measured using the colorimetric assay described above.

Blood biochemistry analysis

Serum TG and cholesterol concentrations were measured using the colorimetric assays described above. Serum alanine aminotransferase (ALT) activity and total bilirubin (#A7526 and #B7576 respectively, Pointe Scientific) were measured by using commercially available kits following the manufacturer’s instruction.

Histology and immunohistochemistry

Livers were fixed in 10% neutral formalin followed by paraffin embedding. Paraffin-embedded liver sections (5 μm) were stained with hematoxylin and eosin (H&E) for pathological evaluation. Immunostaining for F4/80 positive macrophages and myeloperoxidase (MPO) positive neutrophils was performed. TUNEL staining was performed as described previously[3].

Oil Red O staining

Oil Red O staining was performed using liver cryo-sections as described previously[4]. Livers were fixed in 4% paraformaldehyde overnight at 4ºC, infiltrated with 20% sucrose overnight at 4ºC, and embedded in Tissue-Tek OCT Compound. Sections (6 μm) were stained with Oil Red O in 60% isopropanol for 15 min at 37ºC, followed by a 60% isopropanol wash and three washes with water, staining with hematoxylin, and a final wash with water.

Hepatic hydroxyproline measurement

Hepatic hydroxyproline measurement was performed using hydroxyproline assay kit (#K555, BioVision, Milpitas, CA) following the manufacturer's instruction. Briefly, 10 mg liver tissue in 100 μl H_2O was homogenized followed by adding 100 μl 12N HCl and hydrolyzing at 120ºC for 3 hrs. 10 μl of the hydrolyzed liver homogenates were added to a transparent 96-well flat well plate with 100 μl of the Chloramine T reagent and incubated at room temperature for 5 min. 100 μl of the DMAB reagent was then added to each well and incubated for 90 min at 60°C. The absorbance at 560 nm was measured by Tecan plate reader.

Immunofluorescent staining

Immunofluorescent staining was performed using liver cryo-sections as described previously[5]. In brief, cryosections were washed with PBS, blocked with 10% goat serum in PBS with 0.1% Triton X-100 for 30 min, and incubated with primary antibodies overnight at 4ºC, followed by three times PBS wash and incubation with fluorescent-labeled secondary antibodies for 1 hour at room temperature. For staining of neutral lipids and nuclei, samples were incubated with LipidTOX Red and Hoechst 33342 in PBS for 30 min and washed three times with PBS. The coverslips were mounted with antifade reagents (Thermo Fisher). The samples were viewed using a confocal laser microscope (Nikon) and captured with metafluo software.

Electron microscopy

Electron microscopy was performed as described previously[6]. Briefly, livers were perfused with 2.5% glutaraldehyde in 0.1M sodium cacodylate buffer and cut into small pieces. For primary hepatocytes, cells were cultured on plastic coverslips and fixed with 2.5% glutaraldehyde in 0.1M sodium cacodylate buffer overnight, dehydrated and embedded in Epon 812 according to standard procedure. Ultra-thin sections were stained with uranyl acetate and lead citrate and observed using a JEM 1016CX electron microscope (JEOL).

Immunoblot analysis

Total liver proteins were extracted using RIPA buffer (1% NP40, 0.5% sodium deoxycholate, 0.1% sodium dodecyl (lauryl) sulfate in phosphate buffered saline). Protein (30 µg) was separated on a SDS-PAGE gel and transferred to a PVDF membrane. Membranes were probed with appropriate primary and secondary antibodies and visualized with SuperSignal plus chemiluminescent substrate (Thermo

Fisher Scientific). Densitometry analysis was performed with the Un-Scan-It software and normalized to β-actin or GAPDH. All densitometry data are presented as mean ± SEM.

Quantitative real-time polymerase chain reaction (qRT-PCR)

RNA was extracted from mouse liver using Trizol (Thermo Fisher Scientific) and reverse transcribed into cDNA by RevertAid H minus reverse transcriptase (Thermo Fisher Scientific)[7]. Real-time PCR was performed on a Bio-Rad CFX384™ real-time PCR detection system using SYBR® Green mix (Bimake, Houston, TX). Expression of *Acca, Acox1, Acta2, Adgre, Apob, Cd68, Chop, Col1a1, Cpt1a, Crot, Ctgf, Fasn, Gpat1, Hmgcr, Il1β, Il6, Insig1, Insig2, Mcad, Mcp1, Mip1a, Mip1b, Pgc1a, Scd1, Srebp1c, Srebp2, Tgfb1, Tnfα, Xbp1s,* and *Xbp1u,* was quantified using qRT-PCR analysis and *Actb* was used as an internal control. The fold change of mRNA was expressed as $2^{-\Delta\Delta Ct}$. Primer sequences are listed in CTAT table.

Primary hepatocytes culture

Murine hepatocytes were isolated by a retrograde, non-recirculating perfusion of livers with 0.05% Collagenase Type IV (Sigma) as described previously[8]. Cells were cultured in William's medium E supplemented with 10% fetal bovine serum for 2 hours to allow for attachment and then switched to the same medium without FBS. All cells were maintained in a 37°C incubator with 5% CO_2.

Caspase activity measurement

Caspase-3 activities were performed. Briefly, 15 μg total protein was combined with 2 μM Ac-IETD-AFC or Ac-DEVD-AFC (Enzol) in a caspase assay buffer containing

100mM NaCl, 1 mM EDTA, 20 mM PIPES, 10% (w/v) sucrose, 0.1% (w/v) CHAPS, 10 mM dithiothreitol, PH 7.2 in a final volume of 200 µl and incubated for 2 hours at 37°C. The change of fluorescence was measured by a Tecan plate reader.

Metabolomics and lipidomics analysis

Metabolomics and lipidomics of mouse liver tissues were performed at Metabolon, Inc. (Durham, NC). Briefly, for metabolomic analysis, liver samples were prepared using the automated MicroLab STAR® system from Hamilton Company. After protein removal, the resulting extract was divided into five fractions: two for analysis by two separate reverse phase (RP)/UPLC-MS/MS methods with positive ion mode electrospray ionization (ESI), one for analysis by RP/UPLC-MS/MS with negative ion mode ESI, one for analysis by HILIC/UPLC-MS/MS with negative ion mode ESI, and one sample was reserved for backup. Raw data was extracted, peak-identified and QC processed using Metabolon's hardware and software. For lipidomic analysis, lipids were extracted from samples in methanol:dichloromethane in the presence of internal standards. The extracts were concentrated under nitrogen and reconstituted in 0.25 mL of 10 mM ammonium acetate dichloromethane:methanol (50:50). The extracts were transferred to inserts and placed in vials for infusion-MS analysis, performed on a Shimazdu LC with nano PEEK tubing and the Sciex SelexIon-5500 QTRAP. The samples were analyzed via both positive and negative mode electrospray. The 5500 QTRAP scan was performed in MRM mode with the total of more than 1,100 MRMs. Individual lipid species were quantified by taking the peak area ratios of target compounds and their assigned internal standards, then multiplying by the concentration of internal standard added to the sample. Lipid class concentrations were calculated from the sum of all

molecular species within a class, and fatty acid compositions were determined by calculating the proportion of each class comprised by individual fatty acids. Statistical analysis was performed using ArrayStudio, R (http://cran.r-project.org/) or JMP. Statistical significance was determined using one-way ANOVA. False discovery rate (FDR) was estimated using q values to account for multiple comparisons.

Transcriptome analysis

Transcriptome analysis of mouse liver tissues from hepatocyte deletion of Vmp1 and their matched WT were used for total RNA sequencing. Sequencing was performed by Stowers Institute for Medical Research Sequencing Facility. Total RNA was extracted from mouse liver tissues using Trizol™ following manufacturer's instructions (Thermo Fisher). Extracted RNA was analyzed with the Agilent 2100 Bioanalyzer system (Agilent Biotechnologies, Palo Alto, CA). cDNA libraries were generated from high quality RNA and sequenced as 75bp single reads on Illumina NextSeq 500 machine (Illumina, San Diego, CA). Raw reads were then demultiplexed into Fastq format allowing up to one mismatch. Reads were aligned to UCSC genome mm10 with STAR aligner (version STAR_2.6.1c), using Ensembl 96 gene models. TPM values were generated using RSEM (version v1.3.0). Pairwise differential expression analysis was performed using R package edgeR between the control and treatment group. GO term enrichments and KEGG pathway analysis/visualization were done based on upregulated and downregulated DE genes using R package GOstats.

Indirect calorimetry analysis

Energy metabolism was assessed in male mice both 2 weeks and 4 weeks post-injection of either AAV8-TBG-null or AAV8-TBG-cre for VMP1 for 3 days on chow diet

by measuring VO2 and VCO2 using a Promethion continuous metabolic monitoring system (Sable Systems International, Las Vegas, NV, USA) as described previously [9]. Mouse body composition was assessed at the onset of each round of indirect calorimetry. Body weight and food weight were measured prior to and following the 3 days of data collection. Respiratory quotient was calculated as VCO2/VO2 and energy expenditure was calculated with a modified Weir equation [EE (kcal/hr) = 60*(0.003941*VO2+0.001106*VCO2)]. Total EE was calculated as the daily average rate of energy expenditure for the final day times 24. Resting EE calculations were made from the average rate of EE during the 30-minute period with the lowest daily EE as kcal/hr and extrapolated to 24hrs for the final day. Non-resting EE was determined from difference between total EE and resting EE. All_Meters is an assessment of cage activity including gross and fine movements; and is determined using the summed distances calculated from the Pythagoras' theorem that the mouse moved since the previous data point based on XY second by second position coordinates.

Fatty acid β-oxidation

FAO by primary hepatocytes was determined as previously described with minor modifications [10]. 12-well plates were washed with warm PBS, and the cells were incubated with 14C-labeled FAO reaction medium consisting of DMEM-low glucose (Invitrogen), 0.5 uCi/ml ^{14}C-palmitate, 50 uM palmitate, 1% BSA, 1 mM carnitine, and 12.5 mM HEPES (pH~7.4) at 37°C for 3 h in quadruplicate. The ^{14}CO2 was driven from a media aliquot by perchloric acid and trapped in NaOH for determination of complete FAO to CO2. Acid-soluble metabolites (ASMs) was determined from the acidified medium following centrifugation (16,000 g, 4°C). The cells were rinsed with PBS and

lysed with SDS lysis buffer. The protein concentration of the lysate was determined by BCA assay.

TG and APOB secretion *in vivo*

In vivo TG and APOB secretion were determined described previously [11, 12]. The mice were fasted for 4-5 hours followed by the injection via tail vein with 1 mg/g Pluronic™ F-127 and 15 mCi/kg of ^{35}S-methionine labeling mix. Blood samples were collected before injection and every hour for 2 hours. Serum TG was measured as above. 10 µl serum samples from 2 hour after injection of ^{35}S-methionine and Pluronic™ F-127 were subjected to 6% SDS-PAGE. Newly synthesized APOB were quantitated by PhosphorImager analysis.

Subcellular fractionation

Subcellular fractions were extracted as previously described[13]. In brief, mouse livers were homogenized in a cold isolation buffer contains 250mM sucrose, 10mM Tris-Hcl, (PH7.4) with protease inhibitors. Lipid fractions were collected from the tops after a 18,000 × g centrifugation and washed three times with isolation buffer. Pellets and supernatants were resuspended followed by centrifugation at 1,000 × g for 10 min. The supernatant (post-nuclear fraction) was collected and subjected to ultracentrifugation in a SW41Ti rotor at 100,000 × g for 45 min at 4 °C. The supernatants (cytosol fraction) and the pellets (membrane fraction) were collected. Lipid fractions were precipitated with 10% TCA and dissolved in 8M uera buffer. All fraction protein concentration was determined by the BCA assay. Proteins from the membrane and cytosolic fractions (20 µg each) and the lipid droplet proteins (2 µg each) were analyzed by immunoblot analysis.

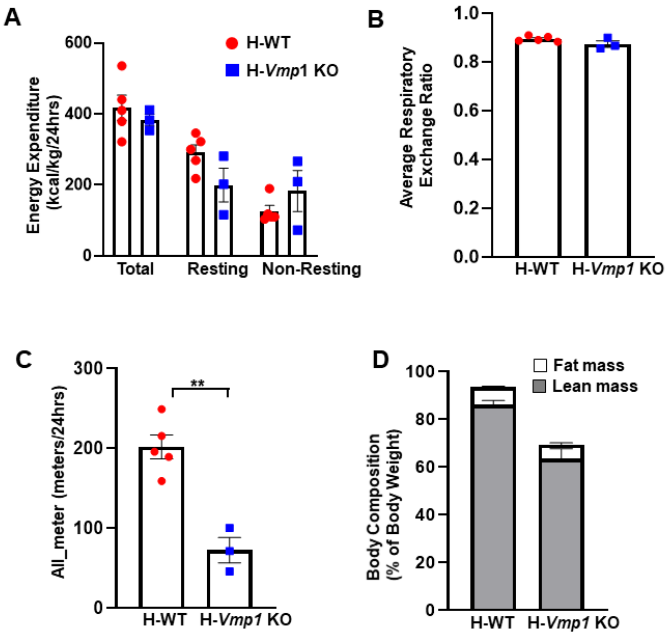

Fig. S1. Indirect calorimetric study of H-Vmp1 KO mice. Male H-*Vmp1* KO and H-WT mice at 4 weeks post AAV injection were subjected to indirect calorimetric study. (A) energy expenditure, (B) average respiratory exchange ratio, (C) activity of all meters and (D) body composition were measured. Data represent mean ± SEM (n=3-5). ** $p<0.01$ (unpaired Student's *t test*).

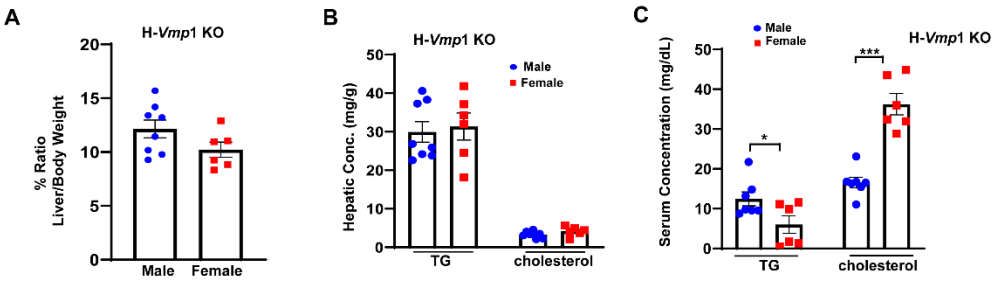

Fig. S2. No gender difference of liver to bodyweight ratio, hepatic steatosis but female mice have lower serum TG but higher serum cholesterol in H-*Vmp1* KO mice. (A) Liver/Body Weight ratio in 8-10 weeks old *Vmp1*^{flox} male and female mice at 2 weeks post AAV8-TBG-cre injection. Hepatic (B) and serum (C) TG and cholesterol were measured in male and female mice fed ad libitum of a chow diet. Data represent mean ± SEM (n=6-8). * $p<0.05$; *** $p < 0.001$ (unpaired Student's *t test*).

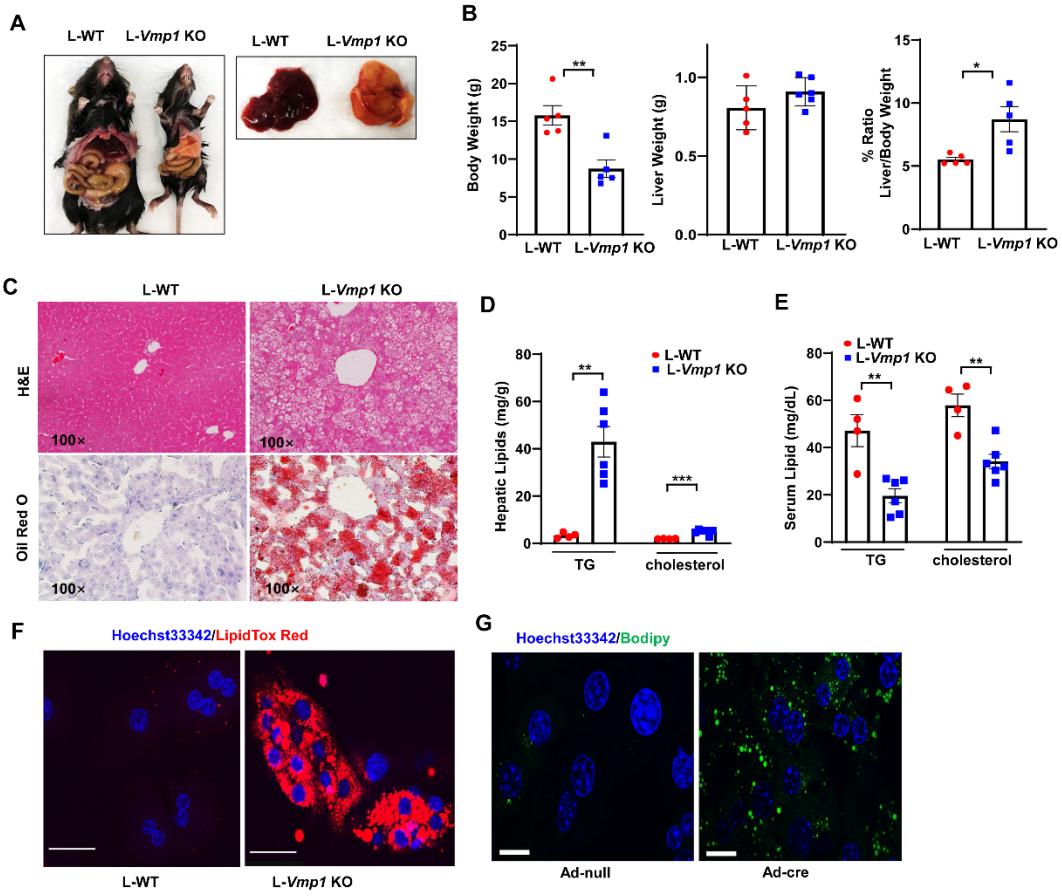

Fig. S3. Liver specific deletion of *Vmp1* in mice causes hepatic steatosis. (A) Representative photograph of mice and livers from Albumin Cre- *Vmp1*^{flox} (L-WT) and Albumin Cre+ *Vmp1*^{flox} (L-*Vmp1* KO) mice at 1 month of age. (B) Body Weight and liver/body weight ratio were quantified. (C) Hematoxylin and eosin staining (H&E) and Oil Red O staining in mouse livers. Scale bars, 100 μm. (D-E) The amount of triglyceride and total cholesterol from livers (D) and sera (E) in L-WT and L-*Vmp1* KO mice fed ad libitum. Primary hepatocytes from L-WT and L-*Vmp1* KO mice (F) or from *Vmp1*^{flox} infected with Ad-null and Ad-cre (G) were stained with LipidTox Red or Bodipy and Hoechst33341 for neutral lipids and nuclei respectively and subjected to confocal microscopy analysis. Scale bar 50 μm. Data represent mean ± SEM (n=4-6). * p<0.05; ** p<0.01; *** p<0.001 (unpaired Student's *t test*).

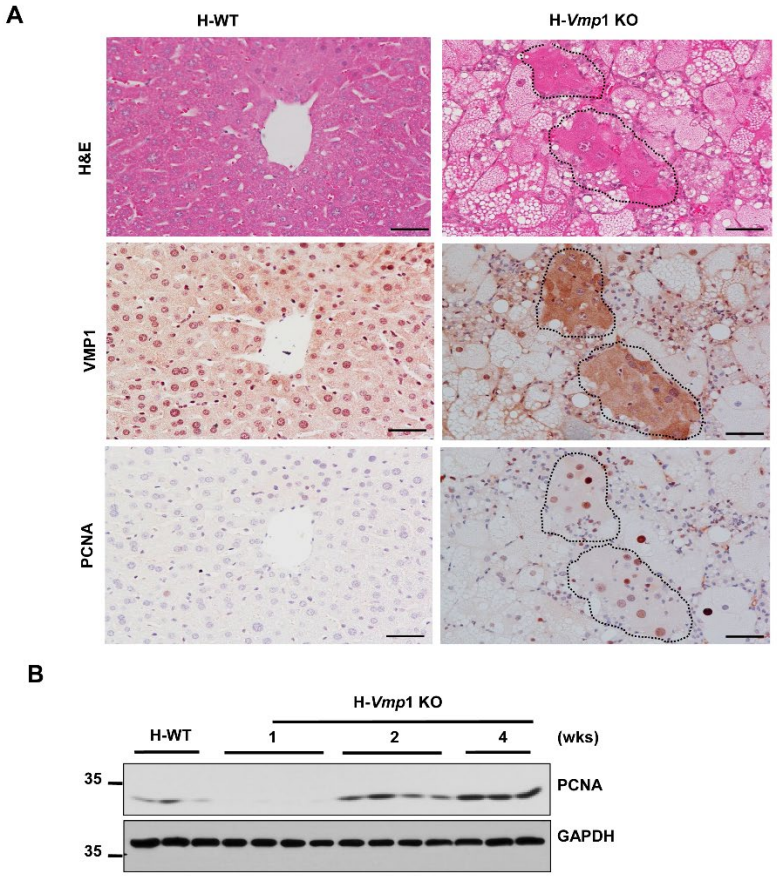

Fig. S4. Hepatocyte proliferation followed by AAV8-TBG-cre injection. (A) Liver sections from H-Vmp1 KO mice at 4 weeks post AAV injections were subjected to H&E staining and IHC for VMP1 and PCNA. Representative images are shown. Dotted areas denote hepatocytes that still express VMP1. Scale bar 50 μm. (B) Total protein lysates were extracted from mouse livers of indicated genotypes and time post AAV injection followed by immunoblot analysis.

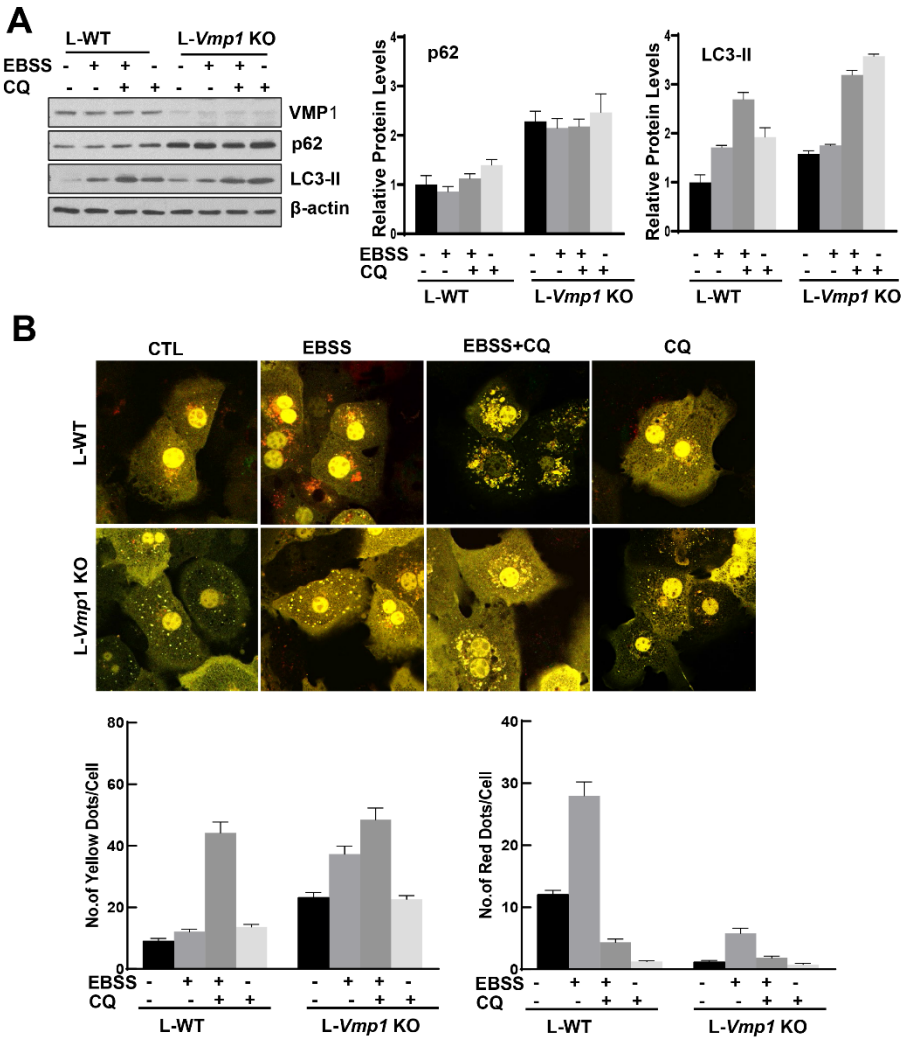

Fig. S5. Defective autophagy in *Vmp1* KO mice. (A) Primary hepatocytes isolated from L-WT and L-*Vmp1* KO mice were treated with EBSS (amino acid starvation) in the presence or absence of chloroquine (CQ, 20 μM) for 2 hours. Total lysates were subjected to immunoblot analysis. The amount of protein was quantified by densitometric analysis. (B) Primary hepatocytes were infected with Ad-*Rfp-Gfp-Cox8* and treated with EBSS in the presence or absence of CQ (20 μM) for 2 hours followed by confocal microscopy. Yellow and red puncta were quantified. The data were from three independent experiments where at least 20 cells were counted from each experiment. Data represent mean ± SEM.

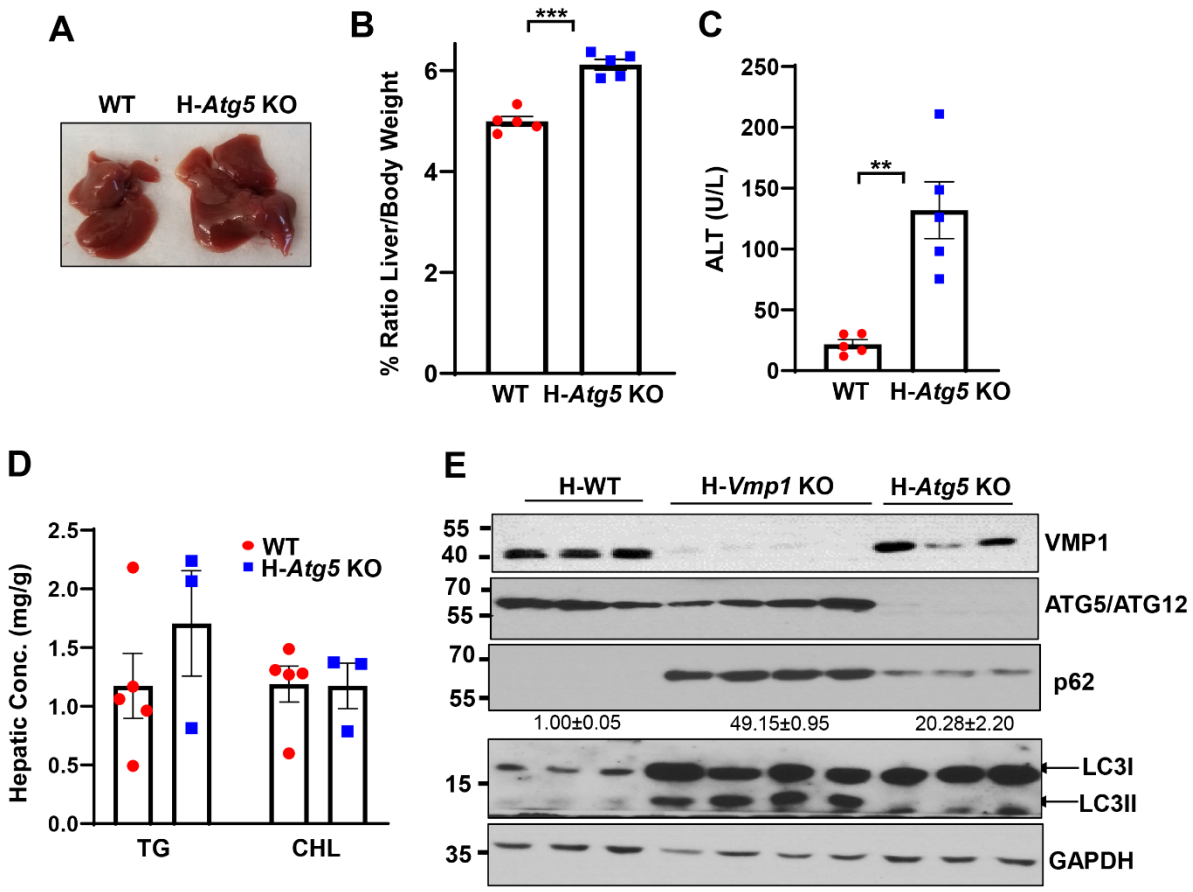

Fig. S6. No lipid accumulation in mice with loss of hepatic Atg5. *Atg5*^{flox} mice were intravenously injected with AAV8-TBG-null or AAV8-TBG-cre for 2 weeks. (A) Representative photograph of mouse livers. Liver/Body Weight ratio (B) and serum levels of ALT (C) were measured. (D) Hepatic TG and cholesterol were analyzed in mouse livers. (E) Total protein lysates were extracted from mouse livers and subjected to immunoblot analysis. Data represent mean ± SEM (n=3-5). ** p<0.01; *** p<0.001 (unpaired Student's *t test*).

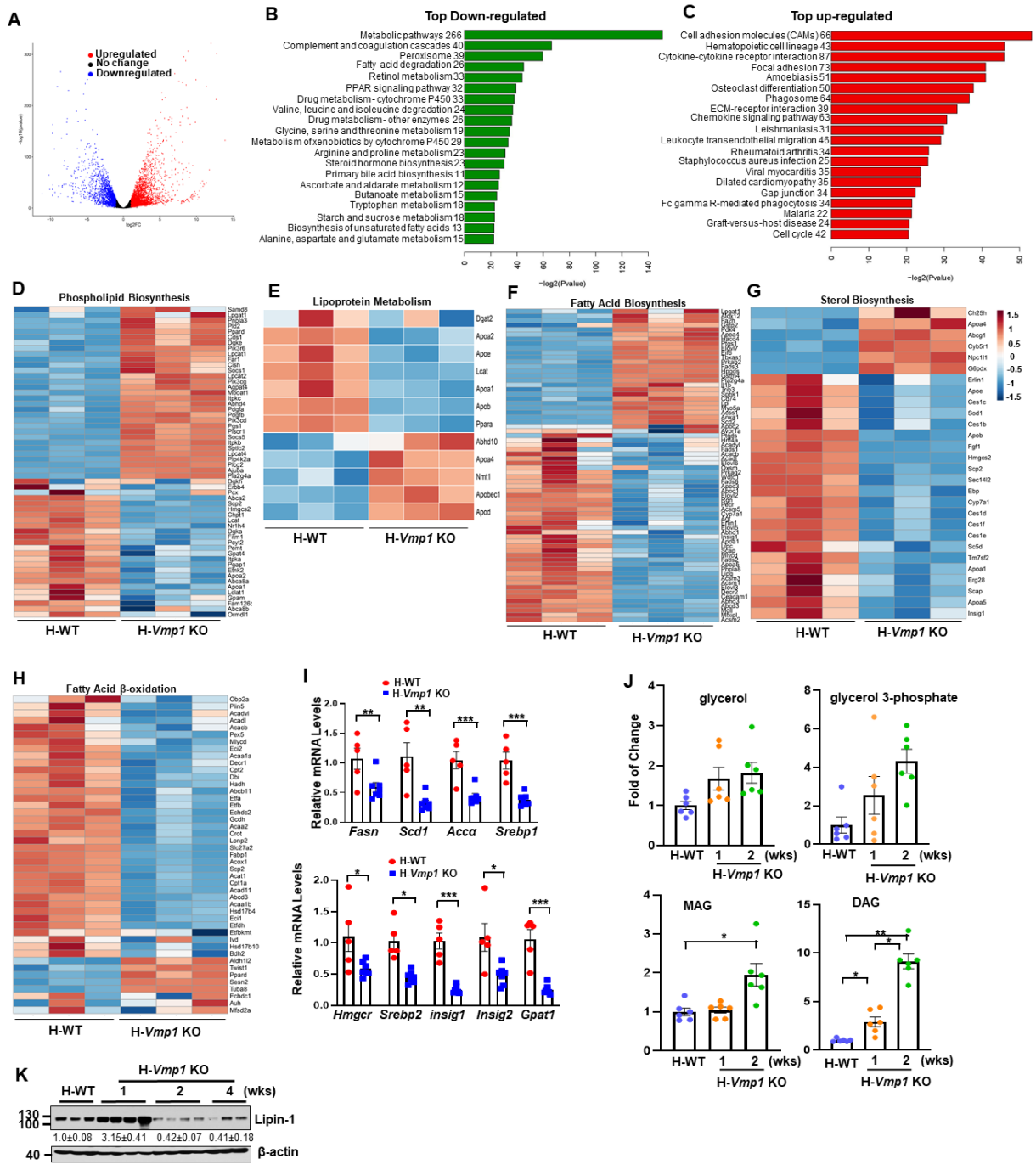

Fig. S7. Transcriptome analysis of hepatic *Vmp1* KO mouse livers. (A) Volcano plots of the RNAseq data of indicated genotypes of mouse livers from H-WT and H-Vmp1 KO mice at weeks post AAV injection (n=3). (B) Top 20 differentially downregulated and (C) Top 20 differentially upregulated pathway-associated gene ontologies of H-Vmp1 KO compared to H-WT mice against statistical significance (represented as ($-\log_2$ p-value) by RNAseq. Heatmaps of phospholipid biosynthesis (D), lipoprotein metabolism (E), fatty acid biosynthesis (F), sterol biosynthesis (G), and fatty acid beta oxidation (H) gene expression from RNAseq analysis. (I) qPCR analysis of the expression of hepatic lipogenesis and cholesterol metabolism genes were

quantified and normalized to *Actb* mRNA. (J) Intermediate metabolites from lipid metabolism were quantified from the metabolomics analysis of indicated genotype of mice. (K) Total liver lysates from the indicated mice were subjected to immunoblot analysis. Data represent mean ± SEM (n=6). * p<0.05; ** p<0.01; *** p<0.001 (Unpaired Student's *t test* or one-way ANOVA with Holm-Sidak post hoc test).

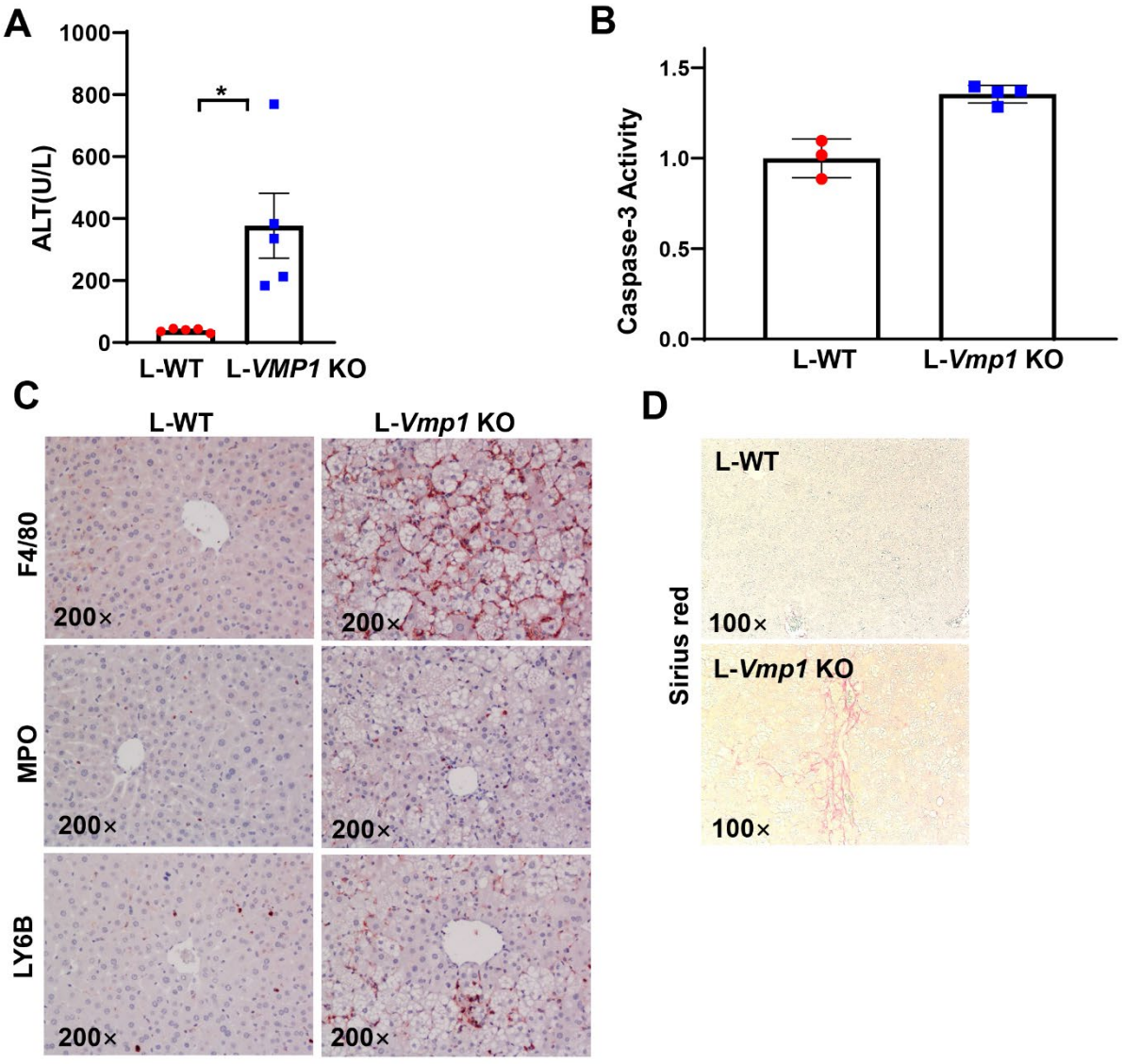

Fig. S8. Liver injury, inflammation and fibrosis in liver specific *Vmp1* KO mice. (A) Serum ALT activity was measured in 1 month old L-WT and L-*Vmp1* KO. (B) Caspase-3 activity was measured in 1-month-old mouse livers. Representative images of IHC staining of F4/80, MPO and LY6B (C) as well as Sirius Red staining (D) from livers of indicated mice are shown. Data represent mean ± SEM (n=4-5). *p<0.05 (Unpaired Student's t test).

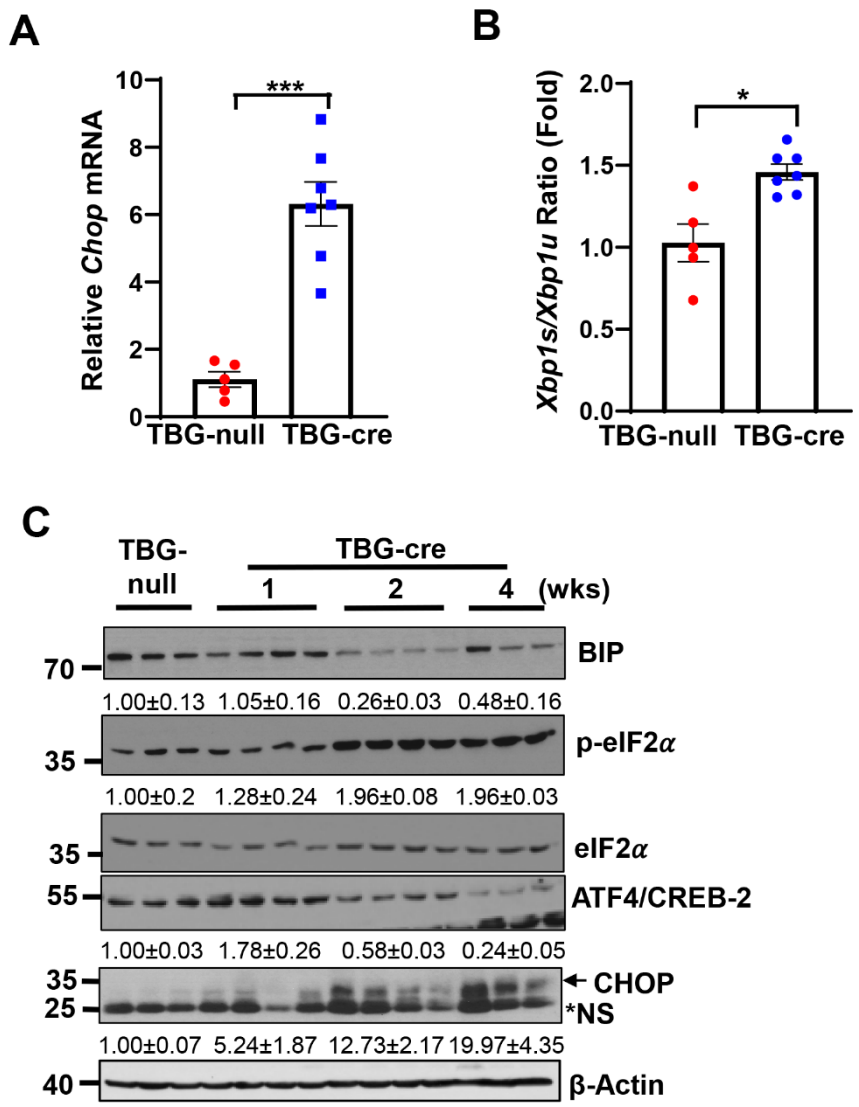

Fig. S9. ER stress in hepatic *Vmp1* deletion mice. (A) ER stress-related gene *Chop* mRNA was detected by qPCR in H-WT *and* H-*Vmp1* KO mice at weeks post AAV injection. Gene mRNA was normalized to *Actb* mRNA. (B) The ratio of XBP1s/XBP1u mRNA level was quantified. (C) Total liver lysate was extracted and subjected to immunoblot analysis. The amount of protein was quantified by densitometric analysis. Data represent mean ± SEM (n=5-7). * p<0.05; ** p<0.01; *** p<0.001 (Unpaired Student's *t test*). NS, non-specific.

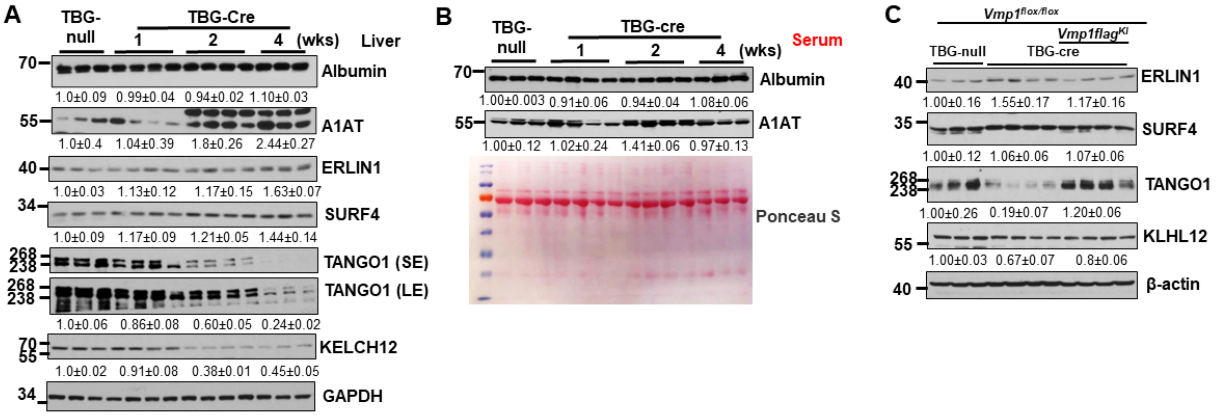

Fig. S10. Loss of hepatic *Vmp1* decreased expression of some transport vesicle proteins but does not affect albumin and apha1 antitrypsin (A1AT) secretion in mice. Total liver lysates (A) and serum (B) from indicated H-WT and H-*Vmp1* KO mice were subjected to immunoblot analysis with the indicated antibodies. (C) Total liver lysates from H-WT, H-*Vmp1* KO and H-*Vmp1* KO/KI mice were subjected to immunoblot analysis with the indicated antibodies.

References

[1] Ni HM, Chao X, Kaseff J, Deng F, Wang S, Shi YH, Li T, Ding WX, Jaeschke H: Receptor-Interacting Serine/Threonine-Protein Kinase 3 (RIPK3)-Mixed Lineage Kinase Domain-Like Protein (MLKL)-Mediated Necroptosis Contributes to Ischemia-Reperfusion Injury of Steatotic Livers. Am J Pathol 2019, 189:1363-74.

[2] Li Y, Chao X, Yang L, Lu Q, Li T, Ding WX, Ni HM: Impaired Fasting-Induced Adaptive Lipid Droplet Biogenesis in Liver-Specific Atg5-Deficient Mouse Liver Is Mediated by Persistent Nuclear Factor-Like 2 Activation. Am J Pathol 2018, 188:1833-46.

[3] Ni HM, McGill MR, Chao X, Du K, Williams JA, Xie Y, Jaeschke H, Ding WX: Removal of acetaminophen protein adducts by autophagy protects against acetaminophen-induced liver injury in mice. J Hepatol 2016, 65:354-62.

[4] Williams JA, Ni HM, Ding Y, Ding WX: Parkin regulates mitophagy and mitochondrial function to protect against alcohol-induced liver injury and steatosis in mice. Am J Physiol Gastrointest Liver Physiol 2015, 309:G324-40.

[5] Ni HM, Chao X, Yang H, Deng F, Wang S, Bai Q, Qian H, Cui Y, Cui W, Shi Y, Zong WX, Wang Z, Yang L, Ding WX: Dual Roles of Mammalian Target of Rapamycin in Regulating Liver Injury and Tumorigenesis in Autophagy-Defective Mouse Liver. Hepatology 2019, 70:2142-55.

[6] Wang S, Ni HM, Chao X, Ma X, Kolodecik T, De Lisle R, Ballabio A, Pacher P, Ding WX: Critical Role of TFEB-Mediated Lysosomal Biogenesis in Alcohol-Induced Pancreatitis in Mice and Humans. Cell Mol Gastroenterol Hepatol 2020, 10:59-81.

[7] Chao X, Wang S, Zhao K, Li Y, Williams JA, Li T, Chavan H, Krishnamurthy P, He XC, Li L, Ballabio A, Ni HM, Ding WX: Impaired TFEB-Mediated Lysosome Biogenesis and Autophagy Promote Chronic Ethanol-Induced Liver Injury and Steatosis in Mice. Gastroenterology 2018, 155:865-79 e12.

[8] Ramachandran A, McGill MR, Xie Y, Ni HM, Ding WX, Jaeschke H: Receptor interacting protein kinase 3 is a critical early mediator of acetaminophen-induced hepatocyte necrosis in mice. Hepatology 2013, 58:2099-108.

[9] Fletcher JA, Linden MA, Sheldon RD, Meers GM, Morris EM, Butterfield A, Perfield JW, 2nd, Rector RS, Thyfault JP: Fibroblast growth factor 21 increases hepatic oxidative capacity but not physical activity or energy expenditure in hepatic peroxisome proliferator-activated receptor gamma coactivator-1alpha-deficient mice. Exp Physiol 2018, 103:408-18.

[10] Morris EM, Meers GM, Booth FW, Fritsche KL, Hardin CD, Thyfault JP, Ibdah JA: PGC-1alpha overexpression results in increased hepatic fatty acid oxidation with reduced triacylglycerol accumulation and secretion. Am J Physiol Gastrointest Liver Physiol 2012, 303:G979-92.

[11] Xie Y, Newberry EP, Young SG, Robine S, Hamilton RL, Wong JS, Luo J, Kennedy S, Davidson NO: Compensatory increase in hepatic lipogenesis in mice with conditional intestine-specific Mttp deficiency. J Biol Chem 2006, 281:4075-86.

[12] Shin JY, Hernandez-Ono A, Fedotova T, Ostlund C, Lee MJ, Gibeley SB, Liang CC, Dauer WT, Ginsberg HN, Worman HJ: Nuclear envelope-localized torsinA-LAP1 complex regulates hepatic VLDL secretion and steatosis. J Clin Invest 2019, 129:4885-900.

[13] Smagris E, Gilyard S, BasuRay S, Cohen JC, Hobbs HH: Inactivation of Tm6sf2, a Gene Defective in Fatty Liver Disease, Impairs Lipidation but Not Secretion of Very Low Density Lipoproteins. J Biol Chem 2016, 291:10659-76.